Bi-Phasic Ag-In-Ga Embedded Elastomer inks for Digitally Printed, Ultra-Stretchable, Multi-layer Electronics

Pedro Alhais Lopes[1]†, *Daniel Félix Fernandes*[1]†, *André F. Silva*[1], *Daniel Green Marques*[1], *Aníbal T. de Almeida*[1], *Carmel Majidi*[1]*, *Mahmoud Tavakoli*[1]*

1. Institute of Systems and Robotics, Department of Electrical Engineering, University of Coimbra, Coimbra, Portugal

2. Integrated Soft Materials Lab, Department of Mechanical Engineering, Carnegie Mellon University, Pittsburgh, PA 15213, USA

† First Co-Authors

*Corresponding Authors Email: Prof. C. Majidi: cmajidi@andrew.cmu.edu, Prof M. Tavakoli: mahmoud@isr.uc.pt

Keywords: Printed stretchable electronics, Soft and Flexible Electronics, Eutectic Gallium Indium Alloy, Conductive stretchable ink, Styrene-isoprene block copolymers (SIS), Styrene block copolymer, Bi-phasic conductive ink, EGaIn-Ag

ABSTRACT

A bi-phasic ternary Ag-In-Ga ink that demonstrates high electrical conductivity, extreme stretchability, and low electromechanical gauge factor (GF) is introduced. Unlike popular liquid metal (LM) alloys like eutectic gallium indium (EGaIn), this ink is easily printable, non-smearing, and bonds strongly to a variety of substrates. Using this ink and a simple extrusion printer, it is shown the ability to perform direct writing of ultrathin, multi-layer, circuits that are highly stretchable (max. strain>600%), have excellent conductivity (7.02×10^5 S m^{-1}), and exhibit only modest gauge factor (0.9) related to the ratio of percent increase in trace resistance with mechanical strain. The ink is synthesized by mixing optimized quantities of EGaIn, Ag microflakes, and styrene-isoprene (SIS) block co-polymers (BCP), which functions as a hyperelastic binder. When compared to the same composite without the EGaIn, the Ag-In-Ga ink shows over one order of magnitude larger conductivity, up to~27x lower gauge factor, and ~5x greater maximum stretchability. No significant change over the resistance of the ink was observed after 1000 strain cycles. Microscopic analysis shows that mixing EGaIn and Ag microflakes promotes the formation of $AgIn_2$ micro particles, resulting in a cohesive bi-phasic ink. The ink can be sintered at room temperature, making it compatible with many heat-sensitive substrates. Using this ink and a simple extrusion printer, it is demonstrated for the first time the ability to perform stencil-free, digital printing of multi-layer stretchable circuits over various substrates, including medical wound dressing adhesives, using simple commercial extrusion based printers.

INTRODUCTION

Stretchable electronics have a wide range of applications, including biomonitoring stickers for wearable computing and electro-physiological data acquisition,[1–5] e-skins for robotics applications,[6–8] e-textiles,[9] flexible displays,[10] and 3D-transferable electronics.[11] Unlike flexible printed circuit, which are commonplace and produced in large volumes (e.g. RFID tags), methods for production-scale fabrication of stretchable circuits are not yet mature. Among materials that are used for stretchable circuits, conductive composites consisting of percolating filler particles in a soft polymer matrix are especially popular and have been extensively investigated for decades. These architectures include spherical micro (μPs) or nanoparticles (NPs)[12] and higher aspect-ratio fillers such as flakes[13,14] or nanowires/nanotubes[15] embedded within a silicone-based elastomer,[16] soft polyurethane[17] or other polymer matrix[18]. These blends can be considered printable substances, since they can be tailor-made in the form of viscous pastes or low viscosity inks, and have been investigated for applications in printed electronics, transparent conductive films, large area electronics, and stretchable electronics.[19] However, despite such progress, conductive composites are still limited in stretchable circuit applications, since they typically exhibit hysteresis and increased electrical resistance when subject to cycle tests.

In recent years, gallium-based liquid metal (LM) alloys, such as eutectic gallium-indium (EGaIn; 75.5 wt.% Ga and 24.5 wt.% In), have been investigated by a growing number of research groups as a promising alternative to conductive, particle-filled elastomer composites. Compared to conductive composites, EGaIn-based circuits typically present a higher conductivity (3.4×10^6 S m^{-1}),[20] greater stretchability (>600%),[21] significantly lower electromechanical gauge factor[13,22–24] and negligible hysteresis.[25] However, despite their functional advantages, liquid metals are challenging to pattern in a versatile and scalable manner. Seminal methods for fabrication of LM-

based circuits include injection into pre-formed microfluidic channels,[13,21,26] elastomer molding,[27] freeze casting,[28] stencil lithography,[29–31] selective wetting,[32,33] reductive patterning,[34,35] contact-based printing,[36] masked deposition,[32] laser patterning,[37,38], UV photolithography,[39] and micro contact printing.[40] A review of some of these methods have been presented in.[38,41] Wetting of gallium-based LM with copper particles was possible with aid of an HCl solution.[42] Direct printed of flexible electronics over paper was shown with Nickel-LM mixture[43]

While promising, these methods for LM patterning often involve many manual steps and can be both time consuming and labor-intensive. Therefore, there has been growing interest in the use of digital fabrication methods for rapid and automated LM printing. Seminal work on printing liquid metal includes syringe-based 3D printing of freestanding LM microstructures[44] and "freeze-printing" over a cold plate.[45] Other attempts included a tapping method using a ballpoint pen filled with LM,[46] a custom printing head for the delivery of LM droplets,[47] LM printing using a pneumatic controlled valve and highly controlled 5 axis stage[48], a modified FDM printer that makes a coaxial extrusion of LM, and a thermoplastic, resulting in deposition of LM filled filament,[49] and a printing solution using nitrogen gas and a custom pinhead for a desktop printer.[50] Moreover, several studies have reported the ability to create stretchable electronics through synthesis and printing of EGaIn nano particles (EGaInNP).[51] While this is an important step toward digitally printed stretchable circuits, these methods require a mechanical or laser based sintering to form the conductive patterns as shown in several works from Kramer´s group.[52–54] Also, liquid metal embedded elastomers were synthesized by mixing LM and elastomer[55], which have application as thermally conductive rubbers but are not electrically conductive when initially synthesized. To form electrically conductive pathways, a mechanical pressure should be applied[56]. Mixing these polymers with Graphene flakes shows that the applied pressure needed to induce

electrical conductivity can be reduced to less than 0.1MPa[57]. Also, a mixture of ethylene vinyl acetate (EVA) and liquid metal, with Ag particles was shown as a stretchable conductor[58] that was printed over a commercial VHB tape. For the best electromechanical performance, the ink should overpass ~150% of strain, so that the EGaIn oxide is ruptured.

In one approach, by mixing nickel particles with the EGaIn, the rheological properties of liquid metal were modified, enabling additive manufacturing of 3D structures.[59,60] EGain-Cu amalgams were as well presented as moldable semi-liquid substance that could be molded, or applied using a painting brush[61], although electromechanical coupling was not studied. In both cases with Cu and Ni fillers, no polymeric matrix, or bonding agent was added to the mixture, thus limiting the adhesion of the amalgams to the substrates. To address this, in one work a layer of PMMA glue was first deposited, followed by roller deposition of a nickel-EGaIn mixture[62]. This method improved the adhesion of the amalgam to the surface, but required an additional step for manual deposition of the glue using a pen or a stencil. Also, the amount of filler in the LM was adjusted to make a soft and dispensable paste. However, as the physical properties of these amalgams before and after deposition are same, i.e. there is no "drying" or polymerization step, they keep their soft and smearing nature, thus the addition of a sealing layer over the circuit is necessary.

In previous works, we have shown that coating trace amount of EGaIn, over non-sintered, non-conductive, printed Ag inks and pastes, result in highly conductive and stretchable (>100% strain) circuits.[11] Circuits are first printed with well-established methods i.e. inkjet or screen printing of Ag based inks /pastes, and are then functionalized by EGaIN coating.[11,63] Unlike other works on liquid metal selective wetting, the resulting Ag-EGaIn circuits are non-smearing, as AgNPs act as a strong anchoring point for the LM. However, the technique for printing these circuits, required four steps of Poly(vinyl alcohol) (PVA) coating, Ag printing, LM coating, and LM dewetting.

While promising, these existing methods fall short of the ultimate goal of creating highly stretchable and electromechanically stable soft circuits with high resolution direct-write using widely-available production-scale extrusion-based printers.

In this work we present a novel bi-phasic Ag-In-Ga ink that is highly conductive and stretchable, and has desirable electromechanical properties similar to LM alloys. However, unlike liquid metals, this ink can be extruded and printed with high resolution with low-cost extrusion printers (Figure 1d, 1e) in a manner similar to particle-filled conductive composites. The ink is prepared by mixing of Ag flakes and EGaIn liquid metal within a SIS hyperelastic binder. The Ag-In-Ga material system exhibits an exceptional combination of fluid-like deformability, the ability to withstand significant tensile strain with only modest increase in electrical resistance, and a solid-like integrity that prevents smearing or marking and allows for robust printing. Such properties arise from the unique amalgamation of three distinct micro structures that include Ga-In droplets that are covered by gallium oxide shell, newly formed Ag-In micro particles that are present around these droplets, and Ag flakes that fully surround the Ag-In and Ga-In amalgams. Circuits printed with this method exhibit high electrical conductivity (7.02×10^5 S m^{-1}), extreme stretchability (strain >600%), a modest gauge factor (90% increase in trace resistance at 100% strain), and moderate change in conductivity after 1000 loading cycles. When EGaIn is removed from the composition, the ink loses its conductivity after 25 cycles of 30% strain and exhibits up to 27× greater gauge factor. To show the potential of this ink in stretchable electronics, we demonstrate printing of multi-layer stretchable circuits through a sequence of printing, polymer lamination, and laser ablation of VIAs (vertical interconnect access).

RESULTS

Ag-EGaIn Biphasic ink synthesis and printing: Referring to Figure 1a, the ink is prepared by first dissolving SIS block Copolymers (BCPs) (Sigma-Aldrich) in a toluene solution. Next, Ag flakes (Silflake, Technic) are added using a planetary mixer (Thinky ARE-250). This is followed by the addition of EGaIn, which results in a shiny ink solution (Figure 1b). See Methods section for more details on the ink synthesis. When the ink comes out of the printing cartridge, it rapidly forms a solid, non-smearing texture (Figure 1c, 1d). When compared to a similar AgSIS inks without addition of the EGaIn, the Ag-In-Ga-SIS ink is over one order of magnitude more conductive (7.02×10^5 S m^{-1}, compared to 4.91×10^4 S m^{-1} for AgSIS sample) (Figure 1f), and presents up to ~27× lower gauge factor (Figure 1g), and over 5× greater maximum stretchability (Figure 2a). We performed cycle tests at 30% strain for 1000 cycles, for both inks. Referring to Figure 1h, after 25 cycles the resistance of the AgSIS ink increases by over 1000×, while AgInGa ink is increased by less than 3× after 1000 cycles. Moreover, the AgInGa ink, presents an extremely modest GF of 0.9 at 100% strain (Fig 2D), which is the lowest gauge factor reported for non-serpentine stretchable electronics so far, based on our recent review article.[25] This low gauge factor, and the ink stability over cycles are both very important factors for correct function of digital circuits, that cannot afford large changes of conductivity under strain.

In order to print multi-layer stretchable circuits, we use a Voltera V-One electronics printer, which prints using a standard extrusion nozzle (Figure 1d, Video S1, S2, S4). We demonstrate printing of stretchable circuits over a variety of substrates, including latex, SIS, and medical-grade oxygen-permeable wound dressing adhesive (Tegaderm 3M), which consists of a thin polyurethane membrane coated with an acrylic adhesive. To print over Tegaderm, we first remove one of the

backing films but leave the other one in place in order to maintain the rigidity of the film. Next, the circuit is printed over the Tegaderm (Figure 1e.i). Afterwards, we remove both linings of a new layer of Tegaderm (Figure 1e.ii), and laminate it over the first layer. Afterwards, we create the VIAs using a CO2 laser (Figure 1e.iii). These three steps can be repeated until all layers of the circuit are printed. For reaching the maximum conductivity, the ink should be cured at the room temperature for 24 hours, but to accelerate the process for multi-layer printing, heating at 60ºC for one hour was used. This heating is provided by the printing bed of the extrusion printer, or an oven can be used. Finally, microchips are bonded to the circuit, either by using an anisotropic conductive film (ECATT 9703, 3M), or by simply using the same AgInGa ink as the bonding material. In this case, we wet the microchips with toluene. Toluene partially dissolves the SIS binder in the ink, which results in bonding of the microchip to the circuit. Figure 1i and 1j shows an example of a fully wireless, battery-free multi-layer circuit, with a near-field communication (NFC) coil that is printed over Tegaderm and transferred over the forearm. The circuit harvests its energy wirelessly through electromagnetic field. When a mobile phone approaches the circuit, it commands the mobile phone to open the SPM-ISR website, and at the same time lights up a light-emitting diode (LED). The two-layer coil in this example, contributes to a higher efficiency in harvesting the energy from the mobile phone (Video S3).

Instead of Tegaderm, other polymers can be applied in the desired thickness, using a thin film applicator. This is the case for the multi-layer circuits of Figure 5b, 5e, which are patterned over an SIS layer.

It is worth referring to the important role of SIS polymer in the ink. Although LM wets many substrates due to the Ga_2O_3 layer, it´s wetting properties depend on the substrate material and surface roughness. Moreover, due to the low viscosity of the LM, high resolution printing with

ordinary extrusion printers has not yet been demonstrated. Particle filled LMs were introduced to modify rheological properties of the LM, to allow digital printing. However, these mixtures suffer from low mechanical integrity and low adhesion to the substrate, and therefore can be easily removed from the substrate by manual wiping. Inclusion of SIS binder contributes to internal binding of the ink and thus improves its mechanical integrity. Therefore, after printing, the ink cannot be removed by manual wiping. In addition, SIS enables the adhesion of the ink to various substrates, thus allowing direct printing over a wide range of substrates. SIS is known as a hyperelastic binder, with excellent elasticity and adhesive properties. Although in this work we used SIS, this can be extended to other Styrenic block copolymers (SBCs) such as SBS and SEBS. These SBCs are made of blocks of distinct polymers in which elasticity and adhesive properties come from the mid-blocks and a strengthening skeleton is provided by the styrene. Due to these properties, and their low cost, they are used in many solvents based adhesives, and as well in hot glues. The amount of the polymer and the solvent in the mixture can be tailored in order to adjust the viscosity of the ink, thereby improving mixing and printing.

Electrical, Electromechanical, and Aging Characterization: In order to establish the electrical and electromechanical properties of the printed inks, we perform a series of characterization studies on samples with a standardized dogbone geometry (Figure S1). To isolate the properties of the printed ink, we did not seal the samples with additional polymer. Referring to Figure 2a, the sample printed with the AgInGa ink can be stretched to over 600% of strain, while exhibiting only a modest increase in relative electrical resistance R/R0. In contrast, the AgSIS sample stops conducting at a maximum of ~130% strain, with a resistance of >1000 Ω, 49× higher than its initial resistance. (See Table S1, and Figure S7 for variations of AgSIS ink).

Figure 2b compares the electromechanical coupling of the AgSIS ink and AgInGa-SIS ink, when subject to 1000 cycles of 30% strain. The resistance of the AgSIS ink rapidly increases to over 100kΩ in 25 cycles while the AgInGa ink remains under 3Ω, after 1000 cycles. Figure 2c demonstrates the effect of the LM addition on the EM coupling of the inks. A liquid metal to Ag weight ratio of 0.6, is enough to enable a significant change in the electromechanical behavior of the samples. However, further improvement is possible with an LM/Ag ratio of 1.9, referring to the Figure 2c inset image. Inks with this higher LM content are also printable and are used for all of the printed circuits presented in this work. Figure 2d shows the electromechanical coupling of a sample that is stretched 10 times sequentially to 30%, 50%, and 100% strains. The resistance of the AgInGa traces increases from 1.6 Ω to 3.1 Ω at 100% strain in the last cycle, representing a modest gauge factor of 0.9. Regarding the electrical conductivity of 7.02×10^5 S m^{-1}, this is lower than the pure EGaIn conductivity, which we attribute to the inclusion of the SIS into the composite. The amount of the SIS polymer in the composite may be adjusted to a lower amount if a higher conductivity is desired, however this can affect the electromechanical properties and printability.

In contrast to EGaIn and other liquid metals, the AgInGa ink is non-smearing (Video S1, S8) and does not require encapsulation with a sealing layer. We monitored the electrical and EM properties of the printed circuit over a period of one year, and observed an increase of ~2× times, with a 1.75× increase in the first 6 months (Figure 2e). The conductivity measurement was obtained by analyzing 7 samples from different ink batches. None of the circuits were sealed and all were stored in ambient condition. We performed the same sequence of Figure 2d, 8 months after fabrication of samples and didn't observe any noticeable difference, in terms of electromechanical coupling, when compared to the fresh samples, except for the increase in the initial value of

resistance (Figure 2e). We also studied the behavior of the ink when washed. Samples printed directly over a textile using a stencil were washed in a regular soap solution (see Methods section). The results in Figure 2g show that samples with an initial resistance of ~1Ω increase to ~3.5Ω after 5 washing cycles. Since the initial resistance of the printed ink is quite low, the increase to 3.5Ω is still within an acceptable range for digital circuits.

Microstructure of biphasic composite: Scanning electronic microscopy (SEM) and energy dispersive X-ray spectroscopy (EDS) were used to examine the features and composition of the Ag-In-Ga ink. Referring to Figure 3a, 3b and Figure S3, micrographs of the cross section of the ink and the EDS analysis suggest the presence of microdroplets of Ga-In (~1-10μm) covered by a gallium oxide layer and surrounded by a large quantity of <5μm Ag flakes. In addition to these expected elements (Ga-In and Ag), we also observed formation of intermetallic Ag-In microparticles. These microparticles are approximately the same size as the Ag flakes but are easily distinguishable on account of their spherical shape. It is noticeable that these particles are mostly attached to the borders of the Ga-In droplets. We believe the Ag flakes and AgIn particles act as distributed hinging point that hold the liquid metal droplets in place and prevent them from smearing during surface contact. Figure S2, shows that these particles are composed of 66 wt% of In and 31 wt% of Ag. This corresponds to 28 at% Ag and 56 at% of In, which suggests that these particles are $AgIn_2$. This is consistent with the fact that $AgIn_2$ is usually formed at temperatures lower than 100ºC,[64] above which Ag_2In intermetallic compound is formed. For instance in one work[65], it was found that in thin-films, metals such as Ga, In, and Sn can form intermetallic compounds with Ag at room temperature. They showed that $AgIn_2$ LT (low temperature phase) forms at lower temperature, and between 60 and 120°C this compound transforms into Ag_2In. Figure 3c shows a schematic of the microstructure, based on these analyses.

Another interesting finding from EDS analysis (Figure 3d) is that greater presence of Ga in any location coincides with low concentrations of Ag in these same areas (Figure S4). In contrast, In is distributed throughout the sample, including regions where Ag is also present. In one sense, the high affinity between Ag and In is the reason why Ag flakes act as a strong anchoring point for the EGaIn, thus causing the desired non-smearing behavior. At the same time, the connection between the In and Ga is also critical in giving the trinary metallic system its cohesion and robust deformability. The trinary Ag-In-Ga system is not a new discovery and had been reported for over 5 decades ago.[66] The high affinity between In and Ag has also been well established in previous literature.[67] In this respect, the formation of the Ag-In-Ga system that has been observed in this study is consistent with previous studies, including those that focus on Ag-In bonding. [49-51] Moreover, previous studies have reported that adding indium to Ga induces spatial elemental disorder in the alloy, i.e. indium acts like a "lubricant" at the atomic scale.[68,69] Within the context of soft and stretchable printed electronics, this material system is enabling, since it allows for a combination of fluid-like deformability (necessary to support significant tensile strain) and solid-like integrity to avoid smearing or marking. Finally, we didn't observe a noticeable difference in the microstructure of pristine and stretched samples, as can be observed in Figure S5. This provides further evidence that the composite behaves like an elastic solid in the sense that the microstructure returns to its original state after the material is unloaded.

FULLY PRINTED, UNTETHERED, STRETCHABLE MULTI-LAYER CIRCUITS, SENSORS, AND ANTENNAS

Modern electronics circuits are composed of a combination of electrodes, sensors, interconnects, microchips, and antennas to support wireless energy harvesting, signal processing, and data transmission. Such circuits typically require complex circuit geometries, including multi-layered circuits with z-axis VIAs. While this is a common practice in rigid and flexible PCBs, achieving the same level of complex multi-layered circuits with stretchable electronics remains a challenge. The printing resolution is generally dependent of the printer, and the extrusion setup. With the printer used in this work, we could successfully print line widths and spacing as small as 200µm, over a SIS substrate (Figure 4a, 4c). Figure 4b shows two printed coils over Kapton, with 1mm and 200µm line width. Figure 4d and 4e show optical microscopy images from a pristine sample, and a sample under strain. Using the materials and fabrication techniques introduced in this article, we demonstrate examples of printed circuits, all produced by direct writing of the AgInGa ink. Figure 5a and Video S7 shows a 9×3 matrix of LEDs, printed over a ~300µm SIS layer that remained functional while being subject to repetitive 30% strain cycles. Figure 5b shows an example of a multi-layer circuit printed on an SIS substrate. Here, a SIS layer is produced at the desired thickness using a thin-film applicator, followed by printing, and application of another SIS layer, followed by creation of the VIAs using a CO_2 laser and printing of the second layer of the circuit. Since the ink can be sintered at the room temperature, it can be compatible with heat-sensitive plastics, rubbers, and textile. Figure 5c and 5d demonstrate various examples of printed circuits, art designs, coils, and sensors printed over either an SIS or a Tegaderm medical dressing. Direct printing over a medical-grade adhesive such as Tegaderm, which is breathable and waterproof, represents an important step toward fabrication of on-the-skin medical biomonitoring patches. Video S5, S6, and S7 show printed circuits functionality under strain, including a strain gauge transferred to a volunteer´s wrist (Figure 5d), and a RFID antenna. Figure 5e and Video S6

demonstrate a stretchable printed RFID antenna that harvests energy from an RFID antenna from a distance of 1m and lights an LED without the need for a battery.

CONCLUSIONS

In this work, we have presented materials and methods for digital printing of multi-layer, thin-film circuits that are highly elastic and stretchable. We presented a unique conductive and stretchable ink composed of Ag flakes, liquid Ga-In alloy, and SIS binder that combines the best properties seen in particle-filled conductive composites and liquid metals. The ink presents excellent electrical and electromechanical properties under strain, a very modest gauge factor of 0.9, and a strain limit of over 600%. Moreover, the ink is printable using standard extrusion, is non-smearing, and adheres to a wide range of substrates. The maximum conductivity is achieved when the ink is treated with a curing temperature of 60ºC, thereby making it compatible with heat-sensitive substrates. Using this ink and a simple extrusion-based printer, we demonstrate printing of thin, multi-layer, and stretchable circuits over various substrates. By analyzing the microstructure of the ink, we observed Ga-In droplets, Ag flakes, and $AgIn_2$ microparticles. This trinary system combines solid-like integrity that enables non-smearing and non-marking functionality and fluid-like deformability to support tensile strain.

The AgInGa-SIS ink and extrusion-based printing method represents an important step toward a universal approach for rapid and scalable fabrication of stretchable electronics with complex multilayer circuit architectures. Due to the simplicity, low-cost, and wide-spread use of extrusion-based printers, extrusion printing of a resilient and stretchable ink is an enabling technology for further progress and customization in other fields of research and application. In particular, the AgInGa-SIS ink could be utilized for 3D printed hybrid devices with embedded circuitry, customized e-textile, organ-interfacing bioelectronics, pressure mapping films, soft-robots, and

printed sensors and antennas. It can also enable facile fabrication of customized current collector designs for use in thin-film batteries and energy harvesting systems that are soft, flexible, and stretchable.

MATERIALS AND METHODS

INK SYNTHESIS: The ink is prepared by dissolving SIS in Toluene (15wt% SIS) until a clear solution is obtained. For each 5g of BCP solution, 6.2g of Ag flakes and 15g of EGaIn are added and mixed using a planetary mixer (2000 rpm). Changing the amount of fillers and the ratio between the LM and Ag flakes changes the electrical and electromechanical properties of the ink, as shown in Figure 2.

ELECTRICAL AND ELECTROMECHANICAL CHARACTERIZATION: The Dogbones used were fabricated using the die-C ASTM D412 standard. Dogbones were made by laser patterning (VLS 3.50, Universal Laser Systems Inc) 1mm thick latex films. The films were produced by applying a thin-film applicator to the latex pre-polymer (Elastica PVS Latex) with dimensions presented in Figure S1 (1x50 mm track with 4.0 x 3.5 mm pads). For electromechanical testing, we used an Instron 5969 with a 100N load cell and a data acquisition system composed of a multimeter (gw nstek gdm-8351) and 16-bit DAQ (NI USB 6002). Conductivity measurements are performed at the two square leads of each sample using a desktop multimeter (Fluke 45). The conductivity is calculated from the electrical resistance and the conductance is estimated based on the thickness of the printed samples after cross section analysis with SEM microscopy (**Figure S6**).

EGAIN SYNTHESIS: The LM used was obtained by mixing gallium (75.5wt%) and indium (24.5wt%) in a glass container at 250°C overnight.

PRINTING: Ink cartridges are filled with the AgInGa ink and the printing is performed after, using a Voltera V-One. The settings used are based upon manufacturer guidelines (adapted as needed). To achieve a uniform circuit, usually two layers of ink are required. However, we have also successfully tested 3 and 4 layers in order to achieve better conductivity. After printing, the circuits are usually cured for 45 min in an oven (60°C).

VIAS: VIAs are created using a CO_2 laser (Universal Laser Systems) similar to the method previously described in [70]. Laser parameters should be adjusted based on the substrate. As an example, for Tegaderm we adjusted the percent power and speed.

WASHING TEST: The soap solution (1L of water + 3.5 mL of soap concentrate) was first mixed and poured inside a 5L drum. Samples were put inside the drum and were agitated manually for 30 seconds and settled for 2-3 mins while still inside the soap solution. After this, the samples were washed with rinsing water carefully to remove any remains of the soap solution. Samples were left in the natural environment for 3 hours, letting the moisture evaporate naturally. Resistance measurements were made only when the sample was dried.

SEM MICROSCOPY AND ELEMENTAL ANALYSIS: The surface and cross-section morphologies of the samples were characterized by scanning electron microscopy (SEM) using a FEI Quanta 400FEG ESEM equipped with an EDAX Genesis X4M, which enabled the elemental analysis by Electron Dispersive Spectroscopy (EDS). For the cross-section observation the samples were immersed for 90 seconds in liquid nitrogen. This allowed for a clean fracture of the samples to be made through mechanical impact. The micrographs were collected in secondary electron (SE) and backscattered electron (BSE) modes. Also, EDS surface scanning was used to build the color map of the distribution of the elements (C, Ga, Ag, and In) on the sample's surface.

ASSOCIATED CONTENT

Supporting Information

The supporting information files contain details regarding the characterization of the AgInGaSIS ink, namely SEM and EDS characterization, with focus on EGaIn droplets and $AgIn_2$ formation. The characteristics of the samples for electromechanical characterization are described. The videos show examples of the printing process, examples of applications and smearing tests.
The following files are available:
Supporting Information Figures and Tables (PDF)
Supporting Information Videos (MP4)

AUTHOR INFORMATION

Author information

Corresponding Authors Email: cmajidi@andrew.cmu.edu, mahmoud@isr.uc.pt

Author contributions

The manuscript was written through contributions of all authors. All authors have given approval to the final version of the manuscript. †These authors contributed equally

ACKNOWLEDGEMENTS

This work was partially supported by the Foundation of Science and Technology (FCT) of Portugal through the CMU-Portugal project WoW (Reference Nr: 45913), and Dermotronics (PTDC/EEIROB/31784/2017), financed by the EU structural & investment Funds (FEEI) through operational program of the center region. Funding also came from Add.Additive (POCI-01-0247-FEDER-024533), financed by Regional Development Funds (FEDER), through Programa Operacional Competitividade e Internacionalização(POCI). Access to instruments of TAIL-UC facility, supported by the QREN-Mais Centro program ICT_2009_02_012_1890 is gratefully acknowledged.

ABBREVIATIONS

Gauge Factor (GF)

Eutectic Gallium-Indium (EGaIn)

Liquid Metal (LM)
Styrene-isoprene (SIS)
Block co-polymers (BCP)
Poly(vinyl alcohol) (PVA)
Vertical interconnect access (VIA)
Light-Emitting Diode (LED)
Radio Frequency Identification (RFID)
Nanoparticle (NP)

Microparticle(μP)

Scanning electronic microscopy (SEM)

Energy dispersive X-ray spectroscopy (EDS)

Backscattered electron (BSE)

REFERENCES

(1) Alberto, J.; Leal, C.; Fernandes, C.; Lopes, P. A.; Paisana, H.; de Almeida, A. T.; Tavakoli, M. Fully Untethered Battery-Free Biomonitoring Electronic Tattoo with Wireless Energy Harvesting. *Sci. Rep.* **2020**, *10* (1), 5539. https://doi.org/10.1038/s41598-020-62097-6.

(2) Kim, D. H. Epidermal Electronics (Science (838)). *Science*. 2011, p 1703. https://doi.org/10.1126/science.333.6050.1703-b.

(3) Lopes, P. A.; Vaz Gomes, D.; Green Marques, D.; Faia, P.; Góis, J.; Patrício, T. F.; Coelho, J.; Serra, A.; de Almeida, A. T.; Majidi, C.; Tavakoli, M. Soft Bioelectronic Stickers: Selection and Evaluation of Skin-Interfacing Electrodes. *Adv. Healthc. Mater.* **2019**, *8* (15), 1900234. https://doi.org/10.1002/adhm.201900234.

(4) Leal, C.; Lopes, P. A.; Serra, A.; Coelho, J. F. J.; De Almeida, A. T.; Tavakoli, M. Untethered Disposable Health Monitoring Electronic Patches with an Integrated Ag2O-Zn Battery, a AgInGa Current Collector, and Hydrogel Electrodes. *ACS Appl. Mater. Interfaces* **2020**, *12* (3), 3407–3414. https://doi.org/10.1021/acsami.9b18462.

(5) Carvalho, F. M.; Lopes, P.; Carneiro, M.; Serra, A.; Coelho, J.; De Almeida, A. T.; Tavakoli, M. Nondrying, Sticky Hydrogels for the next Generation of High-Resolution Conformable Bioelectronics. *ACS Appl. Electron. Mater.* **2020**, *2* (10), 3390–3401. https://doi.org/10.1021/acsaelm.0c00653.

(6) Guo, S. Z.; Qiu, K.; Meng, F.; Park, S. H.; McAlpine, M. C. 3D Printed Stretchable Tactile Sensors. *Adv. Mater.* **2017**, *29* (27), 1–8. https://doi.org/10.1002/adma.201701218.

(7) Rocha, R. P.; Lopes, P. A.; De Almeida, A. T.; Tavakoli, M.; Majidi, C. Fabrication and Characterization of Bending and Pressure Sensors for a Soft Prosthetic Hand. *J. Micromechanics Microengineering* **2018**, *28* (3), 034001. https://doi.org/10.1088/1361-6439/aaa1d8.

(8) Rocha, R.; Lopes, P.; De Almeida, A. T.; Tavakoli, M.; Majidi, C. Soft-Matter Sensor for Proximity, Tactile and Pressure Detection. In *IEEE International Conference on Intelligent Robots and Systems*; 2017; Vol. 2017-Septe, pp 3734–3738. https://doi.org/10.1109/IROS.2017.8206222.

(9) Majumder, S.; Mondal, T.; Deen, M. J. Wearable Sensors for Remote Health Monitoring. *Sensors (Switzerland)*. 2017, p 130. https://doi.org/10.3390/s17010130.

(10) Yoon, J.; Joo, Y.; Lee, B.; Oh, E.; Cho, H.; Hong, Y. Stretchable Active-Matrix Light-Emitting Diode Array Using Printed Electric Components on Plastic and Elastomer Hybrid Substrate. In *Digest of Technical Papers - SID International Symposium*; 2018; Vol. 49, pp 1925–1927. https://doi.org/10.1002/sdtp.12475.

(11) Tavakoli, M.; Malakooti, M. H.; Paisana, H.; Ohm, Y.; Green Marques, D.; Alhais Lopes, P.; Piedade, A. P.; de Almeida, A. T.; Majidi, C. EGaIn-Assisted Room-Temperature Sintering of Silver Nanoparticles for Stretchable, Inkjet-Printed, Thin-Film Electronics. *Adv. Mater.* **2018**, *30* (29), 1–7. https://doi.org/10.1002/adma.201801852.

(12) Xu, S.; Zhang, Y.; Cho, J.; Lee, J.; Huang, X.; Jia, L.; Fan, J. A.; Su, Y.; Su, J.; Zhang, H.; Cheng, H.; Lu, B.; Yu, C.; Chuang, C.; Kim, T. Il; Song, T.; Shigeta, K.; Kang, S.; Dagdeviren, C.; Petrov, I.; Braun, P. V.; Huang, Y.; Paik, U.; Rogers, J. A. Stretchable

Batteries with Self-Similar Serpentine Interconnects and Integrated Wireless Recharging Systems. *Nat. Commun.* **2013**, *4*, 1543. https://doi.org/10.1038/ncomms2553.

(13) Park, Y. L.; Majidi, C.; Kramer, R.; Brard, P.; Wood, R. J. Hyperelastic Pressure Sensing with a Liquid-Embedded Elastomer. *J. Micromechanics Microengineering* **2010**, *20* (12), 1–8. https://doi.org/10.1088/0960-1317/20/12/125029.

(14) Carneiro, M. R.; De Almeida, A. T.; Tavakoli, M. Wearable and Comfortable E-Textile Headband for Long-Term Acquisition of Forehead EEG Signals. *IEEE Sens. J.* **2020**, *20* (24), 15107–15116. https://doi.org/10.1109/JSEN.2020.3009629.

(15) Lee, S.; Shin, S.; Lee, S.; Seo, J.; Lee, J.; Son, S.; Cho, H. J.; Algadi, H.; Al-Sayari, S.; Kim, D. E.; Lee, T. Ag Nanowire Reinforced Highly Stretchable Conductive Fibers for Wearable Electronics. *Adv. Funct. Mater.* **2015**, *25* (21), 3114–3121. https://doi.org/10.1002/adfm.201500628.

(16) Muth, J. T.; Vogt, D. M.; Truby, R. L.; Mengüç, Y.; Kolesky, D. B.; Wood, R. J.; Lewis, J. A. Embedded 3D Printing of Strain Sensors within Highly Stretchable Elastomers. *Adv. Mater.* **2014**, *26* (36), 6307–6312. https://doi.org/10.1002/adma.201400334.

(17) Ge, J.; Yao, H. Bin; Wang, X.; Ye, Y. D.; Wang, J. L.; Wu, Z. Y.; Liu, J. W.; Fan, F. J.; Gao, H. L.; Zhang, C. L.; Yu, S. H. Stretchable Conductors Based on Silver Nanowires: Improved Performance through a Binary Network Design. *Angew. Chemie - Int. Ed.* **2013**, *52* (6), 1654–1659. https://doi.org/10.1002/anie.201209596.

(18) Huang, Y.; Zeng, X.; Wang, W.; Guo, X.; Hao, C.; Pan, W.; Liu, P.; Liu, C.; Ma, Y.; Zhang, Y.; Yang, X. High-Resolution Flexible Temperature Sensor Based Graphite-Filled Polyethylene Oxide and Polyvinylidene Fluoride Composites for Body Temperature Monitoring. *Sensors Actuators, A Phys.* **2018**, *278*, 1–10.

https://doi.org/10.1016/j.sna.2018.05.024.

(19) Choi, S.; Han, S. I.; Kim, D.; Hyeon, T.; Kim, D. H. High-Performance Stretchable Conductive Nanocomposites: Materials, Processes, and Device Applications. *Chemical Society Reviews*. Royal Society of Chemistry 2019, pp 1566–1595. https://doi.org/10.1039/c8cs00706c.

(20) Wang, L.; Liu, J. Liquid Metal Inks for Flexible Electronics and 3D Printing: A Review. In *ASME International Mechanical Engineering Congress and Exposition, Proceedings (IMECE)*; American Society of Mechanical Engineers (ASME), 2014; Vol. 2B. https://doi.org/10.1115/IMECE2014-37993.

(21) Mineart, K. P.; Lin, Y.; Desai, S. C.; Krishnan, A. S.; Spontak, R. J.; Dickey, M. D. Ultrastretchable, Cyclable and Recyclable 1- and 2-Dimensional Conductors Based on Physically Cross-Linked Thermoplastic Elastomer Gels. *Soft Matter* **2013**, *9* (32), 7695–7700. https://doi.org/10.1039/c3sm51136g.

(22) Kim, S.; Lee, J.; Choi, B. Stretching and Twisting Sensing with Liquid-Metal Strain Gauges Printed on Silicone Elastomers. *IEEE Sens. J.* **2015**, *15* (11), 6077–6078. https://doi.org/10.1109/JSEN.2015.2462314.

(23) Cooper, C. B.; Arutselvan, K.; Liu, Y.; Armstrong, D.; Lin, Y.; Khan, M. R.; Genzer, J.; Dickey, M. D. Stretchable Capacitive Sensors of Torsion, Strain, and Touch Using Double Helix Liquid Metal Fibers. *Adv. Funct. Mater.* **2017**, *27* (20), 1605630. https://doi.org/10.1002/adfm.201605630.

(24) Wu, Y. H.; Zhen, R. M.; Liu, H. Z.; Liu, S. Q.; Deng, Z. F.; Wang, P. P.; Chen, S.; Liu, L. Liquid Metal Fiber Composed of a Tubular Channel as a High-Performance Strain Sensor. *J. Mater. Chem. C* **2017**, *5* (47), 12483–12491. https://doi.org/10.1039/c7tc04311b.

(25) Fernandes, D. F.; Majidi, C.; Tavakoli, M. Digitally Printed Stretchable Electronics: A Review. *Journal of Materials Chemistry C*. Royal Society of Chemistry (RSC) 2019, pp 14035–14068. https://doi.org/10.1039/c9tc04246f.

(26) Kim, Y.; Zhu, J.; Yeom, B.; Di Prima, M.; Su, X.; Kim, J. G.; Yoo, S. J.; Uher, C.; Kotov, N. A. Stretchable Nanoparticle Conductors with Self-Organized Conductive Pathways. *Nature* **2013**, *500* (7460), 59–63. https://doi.org/10.1038/nature12401.

(27) Gozen, B. A.; Tabatabai, A.; Ozdoganlar, O. B.; Majidi, C. High-Density Soft-Matter Electronics with Micron-Scale Line Width. *Adv. Mater.* **2014**, *26* (30), 5211–5216. https://doi.org/10.1002/adma.201400502.

(28) Fassler, A.; Majidi, C. 3D Structures of Liquid-Phase GaIn Alloy Embedded in PDMS with Freeze Casting. *Lab Chip* **2013**, *13* (22), 4442–4450. https://doi.org/10.1039/c3lc50833a.

(29) Jeong, S. H.; Hagman, A.; Hjort, K.; Jobs, M.; Sundqvist, J.; Wu, Z. Liquid Alloy Printing of Microfluidic Stretchable Electronics. *Lab Chip* **2012**, *12* (22), 4657–4664. https://doi.org/10.1039/c2lc40628d.

(30) Jeong, S. H.; Hjort, K.; Wu, Z. Tape Transfer Atomization Patterning of Liquid Alloys for Microfluidic Stretchable Wireless Power Transfer. *Sci. Rep.* **2015**, *5*, 8419. https://doi.org/10.1038/srep08419.

(31) Lazarus, N.; Bedair, S. S.; Kierzewski, I. M. Ultrafine Pitch Stencil Printing of Liquid Metal Alloys. *ACS Appl. Mater. Interfaces* **2017**, *9* (2), 1178–1182. https://doi.org/10.1021/acsami.6b13088.

(32) Kramer, R. K.; Majidi, C.; Wood, R. J. Masked Deposition of Gallium-Indium Alloys for Liquid-Embedded Elastomer Conductors. *Adv. Funct. Mater.* **2013**, *23* (42), 5292–5296.

https://doi.org/10.1002/adfm.201203589.

(33) Li, G.; Wu, X.; Lee, D. W. Selectively Plated Stretchable Liquid Metal Wires for Transparent Electronics. *Sensors Actuators, B Chem.* **2015**, *221*, 1114–1119. https://doi.org/10.1016/j.snb.2015.07.062.

(34) Khan, M. R.; Bell, J.; Dickey, M. D. Localized Instabilities of Liquid Metal Films via In-Plane Recapillarity. *Adv. Mater. Interfaces* **2016**, *3* (23), 1600546. https://doi.org/10.1002/admi.201600546.

(35) Lu, T.; Finkenauer, L.; Wissman, J.; Majidi, C. Rapid Prototyping for Soft-Matter Electronics. *Adv. Funct. Mater.* **2014**, *24* (22), 3351–3356. https://doi.org/10.1002/adfm.201303732.

(36) Tabatabai, A.; Fassler, A.; Usiak, C.; Majidi, C. Liquid-Phase Gallium-Indium Alloy Electronics with Microcontact Printing. *Langmuir* **2013**, *29* (20), 6194–6200. https://doi.org/10.1021/la401245d.

(37) Lu, T.; Markvicka, E. J.; Jin, Y.; Majidi, C. Soft-Matter Printed Circuit Board with UV Laser Micropatterning. *ACS Appl. Mater. Interfaces* **2017**, *9* (26), 22055–22062. https://doi.org/10.1021/acsami.7b05522.

(38) Joshipura, I. D.; Ayers, H. R.; Majidi, C.; Dickey, M. D. Methods to Pattern Liquid Metals. *Journal of Materials Chemistry C*. 2015, pp 3834–3841. https://doi.org/10.1039/c5tc00330j.

(39) Abbasi, R.; Mayyas, M.; Ghasemian, M. B.; Centurion, F.; Yang, J.; Saborio, M.; Allioux, F. M.; Han, J.; Tang, J.; Christoe, M. J.; Mohibul Kabir, K. M.; Kalantar-Zadeh, K.; Rahim, M. A. Photolithography-Enabled Direct Patterning of Liquid Metals. *J. Mater. Chem. C* **2020**, *8* (23), 7805–7811. https://doi.org/10.1039/d0tc01466d.

(40) Park, M.; Im, J.; Shin, M.; Min, Y.; Park, J.; Cho, H.; Park, S.; Shim, M. B.; Jeon, S.; Chung, D. Y.; Bae, J.; Park, J.; Jeong, U.; Kim, K. Highly Stretchable Electric Circuits from a Composite Material of Silver Nanoparticles and Elastomeric Fibres. *Nat. Nanotechnol.* **2012**, *7* (12), 803–809. https://doi.org/10.1038/nnano.2012.206.

(41) Khondoker, M. A. H.; Sameoto, D. Fabrication Methods and Applications of Microstructured Gallium Based Liquid Metal Alloys. *Smart Materials and Structures*. Institute of Physics Publishing August 8, 2016, p 093001. https://doi.org/10.1088/0964-1726/25/9/093001.

(42) Tang, J.; Zhao, X.; Li, J.; Zhou, Y.; Liu, J. Liquid Metal Phagocytosis: Intermetallic Wetting Induced Particle Internalization. *Adv. Sci.* **2017**, *4* (5), 1700024. https://doi.org/10.1002/advs.201700024.

(43) Chang, H.; Guo, R.; Sun, Z.; Wang, H.; Hou, Y.; Wang, Q.; Rao, W.; Liu, J. Direct Writing and Repairable Paper Flexible Electronics Using Nickel–Liquid Metal Ink. *Adv. Mater. Interfaces* **2018**, *5* (20), 1800571. https://doi.org/10.1002/admi.201800571.

(44) Grosskopf, A. K.; Truby, R. L.; Kim, H.; Perazzo, A.; Lewis, J. A.; Stone, H. A. Viscoplastic Matrix Materials for Embedded 3D Printing. *ACS Appl. Mater. Interfaces* **2018**, *10* (27), 23353–23361. https://doi.org/10.1021/acsami.7b19818.

(45) Gannarapu, A.; Gozen, B. A. Freeze-Printing of Liquid Metal Alloys for Manufacturing of 3D, Conductive, and Flexible Networks. *Adv. Mater. Technol.* **2016**, *1* (4), 1600047. https://doi.org/10.1002/admt.201600047.

(46) Zheng, Y.; He, Z. Z.; Yang, J.; Liu, J. Personal Electronics Printing via Tapping Mode Composite Liquid Metal Ink Delivery and Adhesion Mechanism. *Sci. Rep.* **2014**, *4* (1), 1–8. https://doi.org/10.1038/srep04588.

(47) Li, G.; Wu, X.; Lee, D. W. A Galinstan-Based Inkjet Printing System for Highly Stretchable Electronics with Self-Healing Capability. *Lab Chip* **2016**, *16* (8), 1366–1373. https://doi.org/10.1039/c6lc00046k.

(48) Park, Y. G.; An, H. S.; Kim, J. Y.; Park, J. U. High-Resolution, Reconfigurable Printing of Liquid Metals with Three-Dimensional Structures. *Sci. Adv.* **2019**, *5* (6). https://doi.org/10.1126/sciadv.aaw2844.

(49) Khondoker, M. A. H.; Ostashek, A.; Sameoto, D. Direct 3D Printing of Stretchable Circuits via Liquid Metal Co-Extrusion Within Thermoplastic Filaments. *Adv. Eng. Mater.* **2019**, *21* (7), 1900060. https://doi.org/10.1002/adem.201900060.

(50) Zheng, Y.; He, Z.; Gao, Y.; Liu, J. Direct Desktop Printed-Circuits-on-Paper Flexible Electronics. *Sci. Rep.* **2013**, *3* (1), 1–7. https://doi.org/10.1038/srep01786.

(51) Lin, Y.; Cooper, C.; Wang, M.; Adams, J. J.; Genzer, J.; Dickey, M. D. Handwritten, Soft Circuit Boards and Antennas Using Liquid Metal Nanoparticles. *Small* **2015**, *11* (48), 6397–6403. https://doi.org/10.1002/smll.201502692.

(52) Liu, S.; Yuen, M. C.; White, E. L.; Boley, J. W.; Deng, B.; Cheng, G. J.; Kramer-Bottiglio, R. Laser Sintering of Liquid Metal Nanoparticles for Scalable Manufacturing of Soft and Flexible Electronics. *ACS Appl. Mater. Interfaces* **2018**, *10* (33), 28232–28241. https://doi.org/10.1021/acsami.8b08722.

(53) Mohammed, M. G.; Kramer, R. All-Printed Flexible and Stretchable Electronics. *Adv. Mater.* **2017**, *29* (19), 1604965. https://doi.org/10.1002/adma.201604965.

(54) Liu, S.; Reed, S. N.; Higgins, M. J.; Titus, M. S.; Kramer-Bottiglio, R. Oxide Rupture-Induced Conductivity in Liquid Metal Nanoparticles by Laser and Thermal Sintering. *Nanoscale* **2019**, *11* (38), 17615–17629. https://doi.org/10.1039/c9nr03903a.

(55) Kazem, N.; Hellebrekers, T.; Majidi, C. Soft Multifunctional Composites and Emulsions with Liquid Metals. *Advanced Materials*. July 2017, p 1605985. https://doi.org/10.1002/adma.201605985.

(56) Fassler, A.; Majidi, C. Liquid-Phase Metal Inclusions for a Conductive Polymer Composite. *Adv. Mater.* **2015**, *27* (11), 1928–1932. https://doi.org/10.1002/adma.201405256.

(57) Saborio, M. G.; Cai, S.; Tang, J.; Ghasemian, M. B.; Mayyas, M.; Han, J.; Christoe, M. J.; Peng, S.; Koshy, P.; Esrafilzadeh, D.; Jalili, R.; Wang, C. H.; Kalantar-Zadeh, K. Liquid Metal Droplet and Graphene Co-Fillers for Electrically Conductive Flexible Composites. *Small* **2020**, *16* (12), 1903753. https://doi.org/10.1002/smll.201903753.

(58) Wang, J.; Cai, G.; Li, S.; Gao, D.; Xiong, J.; Lee, P. S. Printable Superelastic Conductors with Extreme Stretchability and Robust Cycling Endurance Enabled by Liquid-Metal Particles. *Adv. Mater.* **2018**, *30* (16), 1706157. https://doi.org/10.1002/adma.201706157.

(59) Daalkhaijav, U.; Yirmibesoglu, O. D.; Walker, S.; Mengüç, Y. Rheological Modification of Liquid Metal for Additive Manufacturing of Stretchable Electronics. *Adv. Mater. Technol.* **2018**, *3* (4), 1–9. https://doi.org/10.1002/admt.201700351.

(60) Votzke, C.; Daalkhaijav, U.; Menguc, Y.; Johnston, M. L. 3D-Printed Liquid Metal Interconnects for Stretchable Electronics. *IEEE Sens. J.* **2019**, *19* (10), 3832–3840. https://doi.org/10.1109/JSEN.2019.2894405.

(61) Tang, J.; Zhao, X.; Li, J.; Guo, R.; Zhou, Y.; Liu, J. Gallium-Based Liquid Metal Amalgams: Transitional-State Metallic Mixtures (TransM2ixes) with Enhanced and Tunable Electrical, Thermal, and Mechanical Properties. *ACS Appl. Mater. Interfaces* **2017**, *9* (41), 35977–35987. https://doi.org/10.1021/acsami.7b10256.

(62) Guo, R.; Sun, X.; Yao, S.; Duan, M.; Wang, H.; Liu, J.; Deng, Z. Semi-Liquid-Metal-(Ni-EGaIn)-Based Ultraconformable Electronic Tattoo. *Adv. Mater. Technol.* **2019**, *4* (8), 1900183. https://doi.org/10.1002/admt.201900183.

(63) Silva, A. F.; Paisana, H.; Fernandes, T.; Góis, J.; Serra, A.; Coelho, J. F. J.; de Almeida, A. T.; Majidi, C.; Tavakoli, M. High Resolution Soft and Stretchable Circuits with PVA/Liquid-Metal Mediated Printing. *Adv. Mater. Technol.* **2020**, *5* (9), 2000343. https://doi.org/10.1002/admt.202000343.

(64) Chuang, T. H.; Huang, Y. T.; Tsao, L. C. AgIn2/Ag2In Transformations in an In-49Sn/Ag Soldered Joint under Thermal Aging. *J. Electron. Mater.* **2001**, *30* (8), 945–950. https://doi.org/10.1007/BF02657715.

(65) Simić, V.; Marinković, Ž. Room Temperature Interactions in Ag-Metals Thin Film Couples. *Thin Solid Films* **1979**, *61* (2), 149–160. https://doi.org/10.1016/0040-6090(79)90457-7.

(66) Campbell, A. N.; Reynolds, W. F. THE SYSTEM SILVER–INDIUM–GALLIUM. *Can. J. Chem.* **1962**, *40* (1), 37–45. https://doi.org/10.1139/v62-007.

(67) Orr, R. L.; Hultgren, R. Heats of Formation of α-Phase Silver-Indium Alloys. *Journal of Physical Chemistry*. American Chemical Society February 1961, pp 378–380. https://doi.org/10.1021/j100820a510.

(68) Yu, S.; Kaviany, M. Electrical, Thermal, and Species Transport Properties of Liquid Eutectic Ga-In and Ga-In-Sn from First Principles. *J. Chem. Phys.* **2014**, *140* (6), 064303. https://doi.org/10.1063/1.4865105.

(69) Daeneke, T.; Khoshmanesh, K.; Mahmood, N.; De Castro, I. A.; Esrafilzadeh, D.; Barrow, S. J.; Dickey, M. D.; Kalantar-Zadeh, K. Liquid Metals: Fundamentals and Applications

in Chemistry. *Chemical Society Reviews*. Royal Society of Chemistry June 7, 2018, pp 4073–4111. https://doi.org/10.1039/c7cs00043j.

(70) Green Marques, D.; Alhais Lopes, P.; De Almeida, A. T.; Majidi, C.; Tavakoli, M. Reliable Interfaces for EGaIn Multi-Layer Stretchable Circuits and Microelectronics. *Lab Chip* **2019**, *19* (5), 897–906. https://doi.org/10.1039/c8lc01093e.

Figures

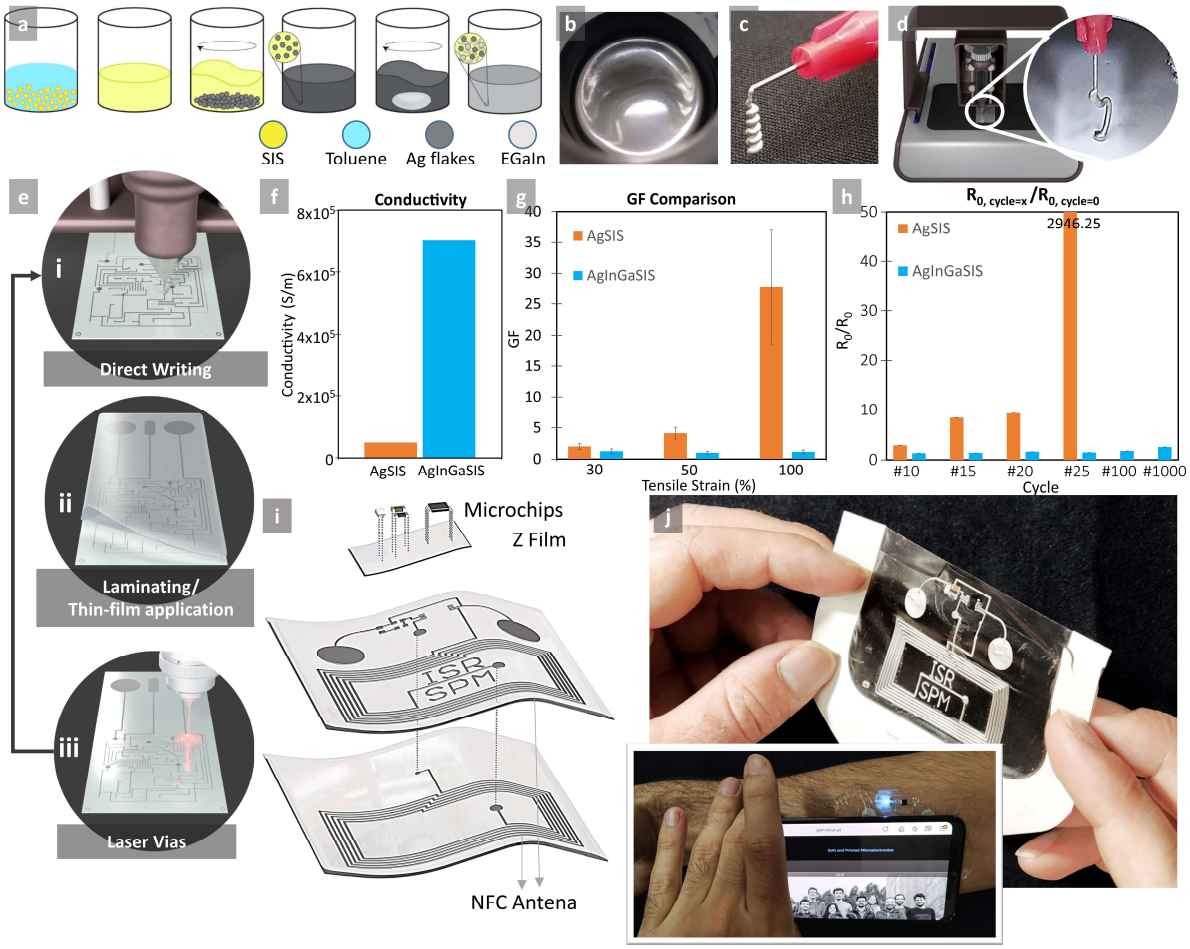

Figure 1. **AgInGa-SIS ink synthesis and printing**. a) The ink is synthesized by first dissolving SIS in toluene, followed by addition and mixing of Ag flakes and EGaIn. b) The final result ink has coherent and shiny appearance. c) The ink rapidly forms a solid structure after coming out of the nozzle. d) A simple extrusion-based printer is used for printing of stretchable inks. Inset shows possibility of extrusion of small free-standing geometries. e) Three fabrication steps for printing multi-layer circuits includes, (i) direct writing (digital printing), (ii) laminating a layer of pre-fabricated polymer, or application of a thin-film of pre-polymer using thin-film applicator. (iii) Electrical VIAs are created using a CO2 laser, or by drilling. These steps can be repeated for making multi-layer circuits. f) Conductivity of AgInGa ink compared to AgSIS ink. g) Gauge factor comparison between the two inks at 30, 50, and 100% strain. h) R0, cycle=x/R0, cycle=0 (0% strain) at different cycles during cycle tests. (i) Representation of a battery-free Multi-Layer NFC circuit, with double layer antenna for high efficiency energy harvesting. Microchips are interfaced to the circuit using an anisotropic conductive film. j) Printed NFC circuit over medical grade Tegaderm adhesive, transferred to the forearm. Inset image: When a mobile phone

approaches the circuit, it lights a LED on the circuit, and opens SPM-ISR website in the mobile phone.

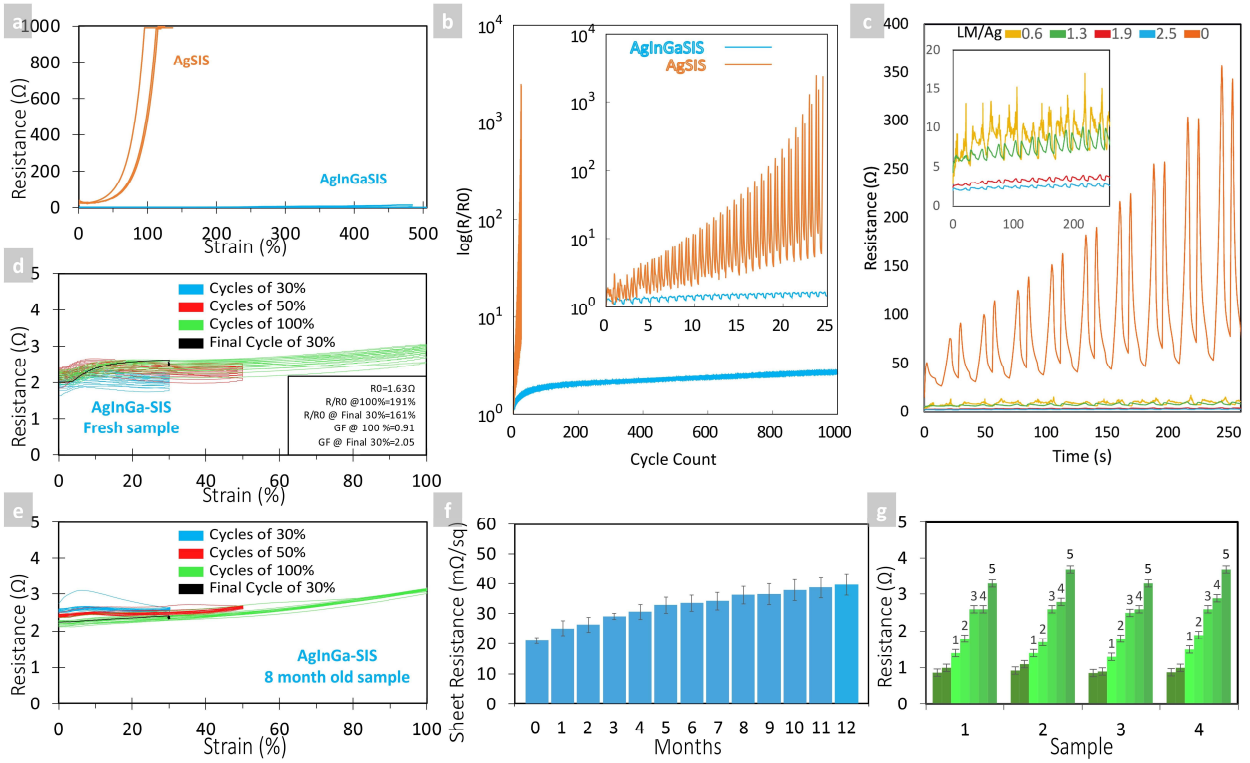

Figure 2. Electrical and Electromechanical Characterization of printed circuits. a) Conductivity vs Strain for the ink with and without the EGaIn. b) Conductivity of both inks during 30% strain cycle tests, for 1000 cycles. c) The effect of the ratio between LM/Ag weight in the ink, with electromechanical coupling characterization of the samples. d) Electromechanical coupling of the AgInGaSIS ink during repetitive 30%, 50%, and 100% strain, and a final cycle of 30% strain. e) Same test for an 8 months old sample. f) Changes on the resistance of unsealed printed samples during one year. Average value from 7 samples from 7 batches. g) Changes on the resistance of 4 samples, after washing them multiple times (number on top of the bar indicates the washing cycle).

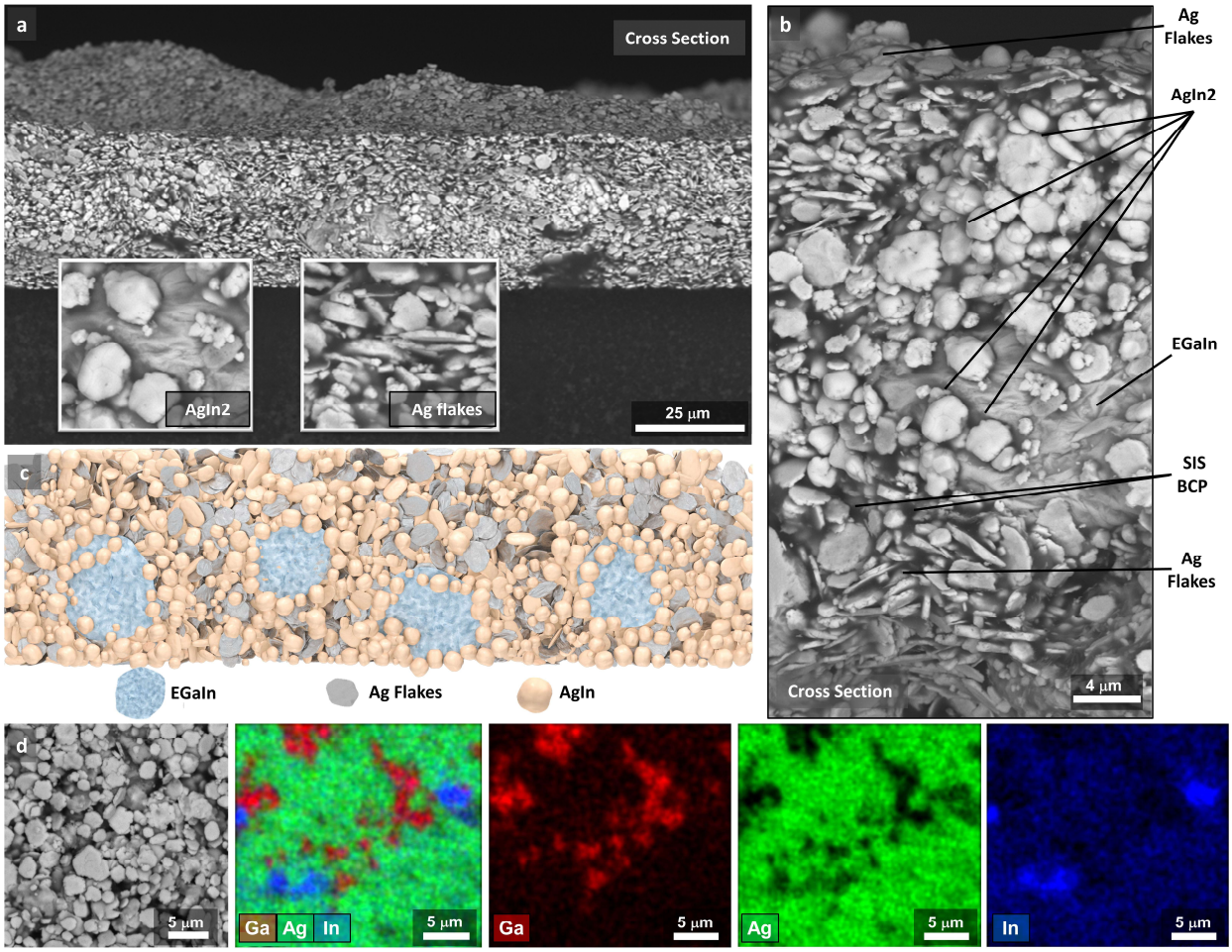

Figure 3. SEM and EDS analysis of ink samples. a) Cross-Section of a printed sample. EGaIn droplets, Ag flakes, and newly formed $AgIn_2$ microparticles are visible (SEM BSE) (25µm scale bar). b) Cross section image at higher magnification, showing EGaIn, Ag microflakes, and $AgIn_2$ (SEM BSE) (4µm scale bar). c) A schematic model of the Trinary microstructure. $AgIn_2$ particles are mostly present around the EGaIn, while the remaining Ag flakes that did not form $AgIn_2$ are distributed in the sample. d) (SEM BSE and EDS) Elemental analysis of the sample, and distribution of Ga, In, and Ag in the microstructure (5 µm scale bars).

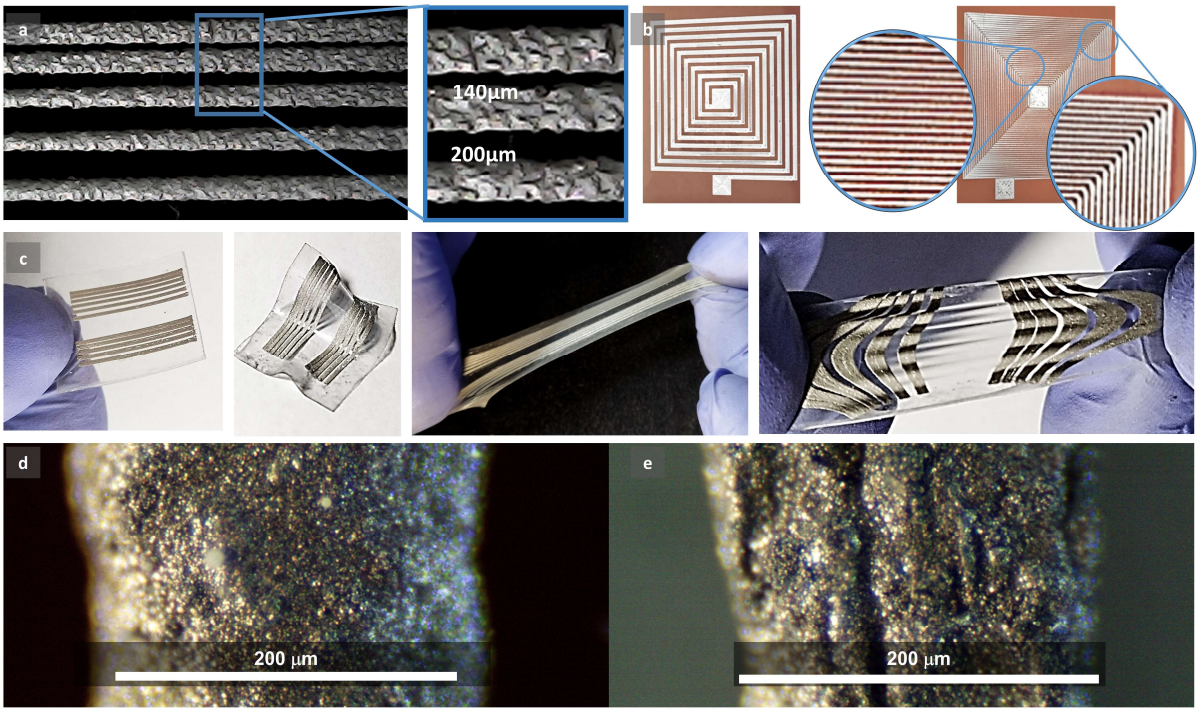

Figure 4. **Printing Resolution.** a) Photo of 200µm Lines printed over a SIS substrate with varying spacing. b) Coils printed over a Kapton substrate with 1mm (left), and 200 µm line width. c) Example of printed lines over SIS layer, and the same sample under stretch (right). d) Optical Microscopy image of a printed line in rest and e) during ~50% strain (200µm scale bars).

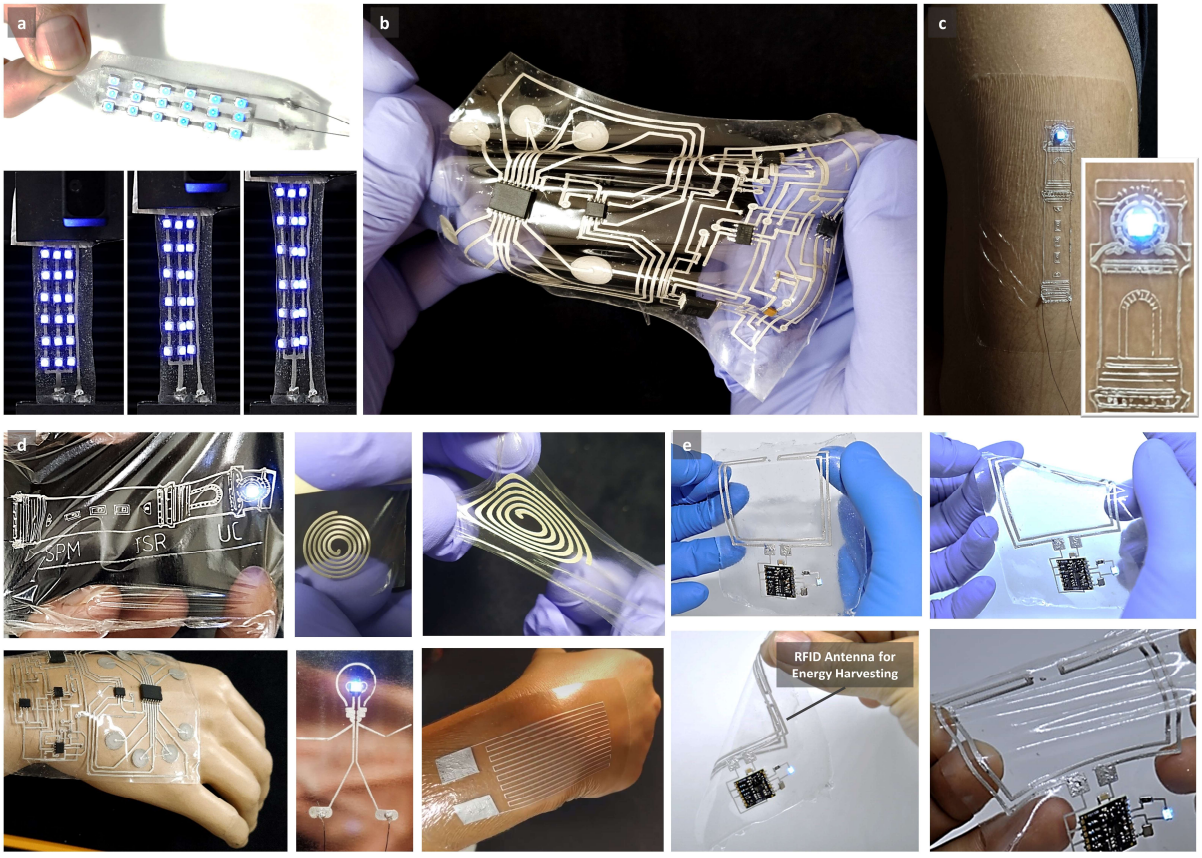

Figure 5. **Examples of digitally printed stretchable circuits.** a) Matrix of LEDs under strain. b) Multi-Layer stretchable circuit made over a SIS substrate. Here, the SIS pre-polymer is applied with a desired thickness, using a thin-film applicator, prior to printing of each layer. c) Circuit printed over Tegaderm medical adhesive and transferred to the skin with LED powered on. d) Examples of various printed circuits, including a strain gauge for monitoring of the wrist bending and a circular coil. e) A fully wireless circuit, composed of a RFID antenna for energy harvesting, a RF to DC module, and a LED, operated at 1m distance from transmitter, without battery.

Table of Contents (TOC)